Vertical Ionization Potentials of Nucleobases in a Fully Solvated DNA Environment

Emilie Cauët,*,†,‡ Marat Valiev,§ and John H. Weare†

Chemistry and Biochemistry Department, University of California San Diego, 9500 Gilman Drive, La Jolla, California 92093, and William R. Wiley Environmental Molecular Sciences Laboratory, Pacific Northwest Laboratories, P.O. Box 999 Richland, Washington 99352

Received: December 22, 2009; Revised Manuscript Received: March 29, 2010

Vertical ionization potentials (IPs) of nucleobases embedded in a fully solvated DNA fragment (12-mer B-DNA fragment + 22 sodium counterions + 5760 water molecules equilibrated to 298 K) have been calculated using a combined quantum mechanical molecular mechanics (QM/MM) approach. Calculations of the vertical IP of the anion Cl^- are reported that support the accuracy of the application of a QM/MM method to this problem. It is shown that the π nucleotide HOMO origin for the emitted electron is localized on the base by the hydration structure surrounding the DNA in a way similar to that recently observed for pyrimidine nucleotides in aqueous solutions (Slavíček, P.; et al. *J. Am. Chem. Soc.* **2009**, *131*, 6460). In a first step, a high level of theory, CCSD(T)/aug-cc-pVDZ, was used to calculate the vertical IP of each of the four single bases isolated in the QM region while the remaining DNA fragment, counterions, and water solvent molecules were included in the MM region. The calculated vertical IPs show a large positive shift of 3.2−3.3 eV compared to the corresponding gas-phase values. This shift is similar for all four DNA bases. The origin of the large increase in vertical IPs of nucleobases is found to be the long-range electrostatic interactions with the solvation structure outside the DNA helix. Thermal fluctuations in the fluid can result in IP changes of roughly 1 eV on a picosecond time scale. IPs of π-stacked and H-bonded clusters of DNA bases were also calculated using the same QM/MM model but with a lower level of theory, B3LYP/6-31G(d=0.2). An IP shift of 4.02 eV relative to the gas phase is found for a four-base-pair B-DNA duplex configuration. The primary goal of this work was to estimate the influence of long-range solvation interactions on the ionization properties of DNA bases rather than provide highly precise IP evaluations. The QM/MM model presented in this work provides an attractive method to treat the difficult problem of incorporating a detailed long-range structural model of physiological conditions into investigations of the electronic processes in DNA.

1. Introduction

The ionization of DNA bases plays an important role in mechanisms of DNA damage caused by ionizing radiation, oxidizing agents, and photoirradiation.[1−3] However, the spectroscopic properties needed to interpret these events are difficult to measure in fully solvated physiologically relevant environments and required data such as the ionization energy thresholds of nucleobases within DNA are not yet available. In lieu of direct observations, there have been numerous experimental[4−26] and theoretical[26−45] investigations directed to the determination of both the vertical and adiabatic ionization potentials (IPs) of the four DNA bases—guanine, adenine, cytosine, and thymine—in the gas phase and in pure aqueous solution. The objective of these studies was to extrapolate these observations to predict the IPs of each of the bases embedded in the DNA solvated helical polymer. However, this extrapolation is not straightforward because it is expected that effects such as base stacking and base pairing and of the covalent attachment of the ribose sugar and the phosphate backbone in double-stranded DNA cause important changes in the electronic structure of the bases and therefore in the IPs.[46−49] In addition, recent calculations of the effects of microsolvation and bulk solvation of DNA bases in water have been shown to be substantial on the electronic structure.[26] Roca-Sanjuán et al.[49] performed QM calculations in conjunction with molecular mechanics on a cytosine inside a 18-base-pair poly(C)−poly(G) surrounded by water molecules showing that the base IP is slightly larger than the gas phase one. These results suggest that the very complex molecular environment of DNA, which has not been observed, may have a significant influence on the base IPs. The objective of our research is to provide estimates of these shifts which we show to be unexpectedly large.

Measurements and calculations have been successful in providing accurate evaluations of the IPs of single DNA bases and some DNA oligomers, in the gas phase and in aqueous solution. The experimental measurements, however, are hindered by a combination of factors including the low photoionization quantum yields of DNA components at physiological pH and the low sensitivity with which aqueous photoionization is detected. Recently, the photophysics properties of nucleosides and nucleotides in water have been investigated.[26] Extensive theoretical calculations of the gas-phase ionization energies of neutral base pairs,[48,50−55] of stacked bases,[42,43,56−61] and of microhydrated base-pair clusters[62−67] have also been reported. The self-consistent polarizable continuum model (i.e., PCM of Tomasi and co-workers[68]) has been widely employed to model the bulk solvent effects on the ionization energy values of the DNA bases in homogeneous aqueous solution isolated and in interaction with the first hydration shell water molecules. Recognizing the limitations of standard PCM models to predict

* To whom correspondence should be addressed. E-mail: ecauet@ulb.ac.be.
† University of California San Diego.
‡ Current address: Service de Chimie Quantique et Photophysique, Université Libre de Bruxelles, CP 160/09, 50 Avenue F. D. Roosevelt, B-1050 Bruxelles, Belgium.
§ Pacific Northwest Laboratories.

10.1021/jp9120723
Published on Web 04/15/2010

vertical spectroscopic events, a nonequilibrium version of a PCM (NEPCM)[69,70] has also been introduced to more accurately account for bulk solvent effects on the ionization of DNA building blocks.[26]

An issue that is of importance to this work and that has received considerable recent attention is the localization in the nucleotides of the molecular orbital from which the electron is removed in the lowest energy ionization process. Recent calculations[71−76] and measurements[71,77] in the gas phase have contributed greatly to the understanding of this process. However, controversial results have been reported and some debate remains. On the basis of DFT B3LYP calculations, Yang et al.[71] suggest that, in a vacuum, the lowest ionization channel is related to the base for 2′-deoxyguanosine 5′-monophosphate ($dGMP^-$) and to the phosphate group for the three other DNA mononucleotide anions: 2′-deoxyadenosine 5′-monophosphate ($dAMP^-$), 2′-deoxycytidine 5′-monophosphate ($dCMP^-$), and 2′-deoxythymidine 5′-monophosphate ($dTMP^-$). On the other hand, the CASPT2 calculations of Rubio et al.[74,76] for both nucleotides $dGMP^-$ and $dTMP^-$ also in the gas phase support the nucleobase as the site of the lowest IP. This is consistent with the P3 results of Zakjevskii et al.[73] which assign the lowest IP for $dTMP^-$ to the thymidine fragment but for $dCMP^-$ and $dAMP^-$ to the phosphate group. According to these authors, only $dGMP^-$ presents a first IP that corresponds to the excitation of the base. New calculations have also been performed on $dAMP^-$, suggesting that if the charge on the phosphate is neutralized by a counterion the ionization occurs on the base.[75] There is evidence that the localization of the hole may be a function of the solvation of the system.[78−80] Recently, direct measurements and calculations of pyrimidine nucleosides in the aqueous phase have shown that the bulk hydration can dramatically change the localization and ordering of the electronic energy levels of these species.[26] These data strongly support the localization of the orbital associated with the lowest IP in the π-structure of the nucleobase. However, none of these studies have attempted to treat the unique solvation environment of DNA. The bases embedded in the solvated DNA helix experience a very different interaction with the solvation shell. Although the immediate environment of the base is essentially anhydrous, the charged DNA helix produces a structured solution that is expected to lead to a large polarization field at the site of the DNA base fragment.

The calculations reported here are based on a combined quantum mechanical molecular mechanics (QM/MM) model in which a realistic representation of the environment surrounding DNA bases that includes atoms of the double helix, counterions, and a discrete representation of water solvent structure is included in the MM region. The species involved in the ionization process of interest constitute the so-called QM region and are treated with high-level quantum chemistry methods. Such QM/MM methods have been quite successful in predicting excited state properties of DNA bases in various environments.[81−83] Several essential points discussed in more detail next in this Article support the development of the QM/MM model to obtain vertical ionization energies of DNA bases. These include the fact that, as we will show below, the polar environment in DNA favors the localization of the orbital origin of the lowest vertical IP for nucleotides on the base. Given the location of ionization on the base and the anhydrous environment kept around the bases by the double helical structure of DNA, this is an ideal QM/MM system. That is, the electronic structure of the nucleobases included in the QM region is isolated from the rest of the system (the MM region). The usual problem with QM/MM separation is, therefore, not an issue. The atoms outside the QM region affect the atoms inside the QM region primarily through long-range electrostatic interactions which are straightforward to calculate within a QM/MM model.

The QM/MM calculations presented in this paper lead to the conclusion that the negative phosphate groups of the DNA double helix and positive counterions induce a long-range molecular structure of the solvent creating, in the center of the DNA helix, an electric potential noticeably amplified. This potential shifts the ionization energy threshold of DNA bases by approximately 3.2−3.3 eV relative to the gas phase. These shifts could not have been anticipated from prior model or aqueous phase simulations. They are found to be larger than the shifts resulting from base pairing, base stacking, or hydration in homogeneous solution and, therefore, are expected to play an important role in the photochemistry of DNA. The QM/MM model has also been applied to IP calculations of clusters of DNA bases. We report here calculations of up to a four-base-pair duplex. The energy shifts due to H-bonding and stacking interactions are consistent with those calculated by others.[47] The important IP shift due to solvation surrounding DNA remains at about the same level as for single DNA bases.

2. Methods of Calculation

2.1. QM/MM Scheme. In order to represent the cumulative effects of the solution structured by the presence of the anionic DNA and the counterions, the system must contain orders of magnitude more atoms than could be included in a first principle calculation. Solvated molecules are commonly treated by embedding in a continuum dielectric, as in the PCM approaches. However, these continuum approaches do not allow the explicit molecular description of the solvent, which is necessary to describe effects such as of the local structure of the solvation shells and the coordination of counterions. In this work, we introduced a QM/MM methodology to retain a molecular view of these effects of hydration while bridging large particle size scales. All of the calculations were performed with the NWChem program suite.[81] In the QM/MM method, the total energy for the entire system is expressed by

$$E = E_{\mathrm{QM}} + E_{\mathrm{QM/MM}} + E_{\mathrm{MM}} \tag{1}$$

where E_{QM} and E_{MM} are the internal energies of the QM and MM regions and are calculated in the standard quantum chemistry and classical molecular ways, respectively. The $E_{\mathrm{QM/MM}}$ contribution contains the interactions between the QM and MM regions and is given by

$$E_{\mathrm{QM/MM}} = \sum_{iM} \int \frac{\rho(\mathbf{r}) q_M}{|\mathbf{r} - \mathbf{R}_M|}\,\mathrm{d}\mathbf{r} + \sum_{IM} \frac{Z_I q_M}{|\mathbf{R}_I - \mathbf{R}_M|} + \sum_{IM} \left\{ \frac{A_{IM}}{|\mathbf{R}_I - \mathbf{R}_M|^{12}} - \frac{B_{IM}}{|\mathbf{R}_I - \mathbf{R}_M|^{6}} \right\} + \sum_{IM} \frac{k}{2} (\mathbf{R}_{IM} - \mathbf{R}^0_{IM})^2 + \ldots \tag{2}$$

The first two terms in the eq 2 describe electrostatic interactions between the electron density, $\rho(r)$, and nuclear charges, Z_I, in the QM region with classical charges, q_M, in the MM region. Here, we are assuming that the long-range interactions in the MM region are described by Coulomb interactions, as typically appears in water−water interaction

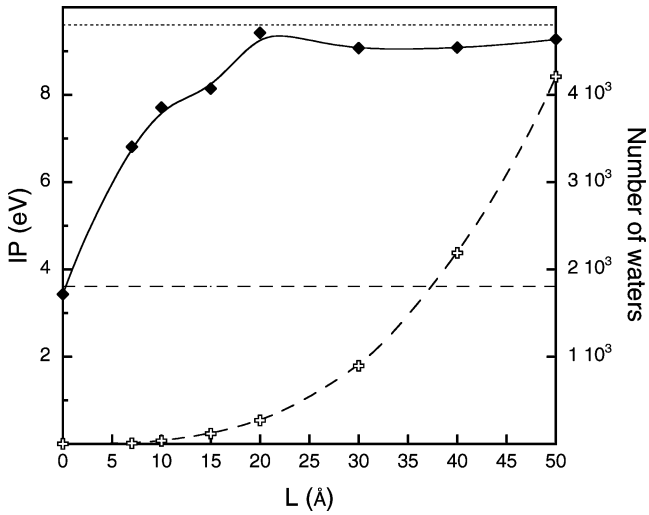

Figure 1. CCSD(T)/aug-cc-pVDZ vertical IP (diamonds) of a Cl^- ion and number of hydrating waters included in each calculation (crosses) as a function of the size of the solvent cubic box (L). The experimental values in the gas phase and solution correspond to the dotted and dashed lines, respectively.

potentials. The third term in eq 2 describes the nonbonded van der Waals interactions and repulsive short-range interactions between the QM and MM regions, while the remaining terms model bonding interactions between the QM and MM regions. Within this QM/MM description, the polarization of the QM system is taken into account by solving the electronic structure problem in the field created by the MM region. The charge distribution of the MM system is determined by the positions of point charges at the MM nuclear coordinates. Electronic polarization in the MM region in response to the QM charge distribution is not treated. In principle, the QM and MM regions will polarize each other until their charge distributions are self-consistent. However, self-consistency is difficult to achieve because it requires a polarizable MM force field, which has the flexibility to respond to perturbation by an external electric field. Such flexibility is not available in most of today's QM/MM models, although research to develop a polarizable force field has received much attention.[84−86] Moreover, the use of a self-consistent scheme also brings additional complication to the treatment of the boundary between the QM and MM regions.[87] In this work, the effect of the polarization of the MM region is expected to be small compared to the effect of the permanent polarization field of the MM waters surrounding the DNA helix. However, in order to estimate the accuracy of the QM/MM method described here for vertical IP calculations, we used this approach to estimate the vertical IP of the Cl^- ion for which experimental values are well established both in gas phase and in aqueous phase.[88,89] For the calculations in solution, the Cl^- anion was embedded into cubic simulation boxes of 7, 10, 15, 20, 30, 40, and 50 Å side containing from 10 up to 4200 water molecules. The SPC/E[90] model was used for water−water interaction and the Amber[91] potential for the water−ion interaction. The systems were equilibrated by classical molecular dynamics (MD) simulation performed at room temperature (298 K) and pressure (1 atm) over 60 ps. Figure 1 presents the vertical IP of the Cl^- anion calculated as a function of the size of the solvent cubic box (L). The number of water molecules implied in each calculation is also depicted. The experimental values in the gas phase and solution correspond to the dotted and dashed lines, respectively. The gas-phase IP of Cl^- obtained with the coupled-cluster of single and double excitations with perturbative triples theory[92] (CCSD(T)) and the aug-cc-pVDZ[93] basis set (3.43 eV) agrees within 0.2 eV with the corresponding experimental value of 3.61 eV. An important change of the IP value is observed between $L = 0$ Å (gas phase) and $L = 20$ Å (269 waters). The QM/MM vertical IP of the fully solvated anion at $L = 50$ Å (4200 waters) is found to be 9.27 eV, also at the CCSD(T)/aug-cc-pVDZ level, and differs by only 0.3 eV from the experimental IP value (9.60 eV) measured in water. We note that the vertical IP values of Cl^- reported for the equilibrium PCM and NECPM calculations (MP2/aug-cc-pVDZ)[94] are 6.63 and 8.55 eV, respectively, well below the experimental value of 9.6 eV. Figure 1 thus clearly demonstrates the sensitivity of the IP with the increasing number of waters surrounding the ion and shows that the long-range solvation effects have to be considered to make the IP converge to the experimental value. This result supports the idea that the water−water interactions are dominant over the ion−water interactions in determining the polarization state of the solvent induced by ions such as Cl^-.[95−97] Zhao et al.[98] have recently showed that, upon full hydration, the average dipole magnitudes for inner-shell waters of the chloride ion are slightly reduced from the bulk value and that the first shell water−water interactions (modified by interactions with the anion) and the H-bonding environment from the second solvation shell are the major factors that determine the polarization of the first shell water molecules. This indicates that, although the QM/MM methodology does not take the solvent polarization explicitly into account, it is very practical to include the large-scale effects of bulk hydration. This treatment appears to provide an accurate estimate of the Cl^- IP in solution and a good estimate of the IP shift (∼6 eV) created by the solvent.

2.2. Simulation Details. Our system consisted of a 12-mer fragment of B-DNA (3′-TCGCGTTGCGCT-5′) with the backbone sugar−phosphate groups neutralized by 22 sodium cations (see Figure 2a). Each strand was terminated with an OH group. We carried out simulations with the system placed in two rectangular boxes of water molecules of different sizes: 51 × 51 × 69 Å with 5760 waters and 105 × 105 × 123 Å with 40 000 waters. Molecular systems of various sizes (from single bases to π-stacked bases and H-bonded base pairs up to four-base-pair duplex) were chosen to be included in the QM region and treated with the quantum chemistry methods described below. The remaining parts of the system were included in the MM region. The linking bonds connecting the QM and MM regions were capped with hydrogen link atoms. The Amber-type force field[91] parameters were used for DNA, while the water molecules were treated using the SPC/E[90] model. This simple three-charge model of water−water interactions has been demonstrated to provide a very satisfactory representation of the structure of water under ambient conditions. In addition, the dielectric properties of pure water which is critical in this research are provided quite accurately by this model, e.g., $\varepsilon_{SPC/E} = 70$ D and $\varepsilon_{exp} = 72$ D for $T = 234$ K.[99]

The entire system was equilibrated by performing a series of MD annealing runs for 60 ps at temperatures of 50, 100, 150, 200, 250, and 298 K. This equilibration process led to a structured solution surrounding the DNA helix in which the positive sodium counterions coordinate the negatively charged phosphate groups of the DNA background, as illustrated in Figure 2b. A feature of this structure that will be important to the following discussion is the almost complete exclusion of water from the inside of the DNA helix. We give in Figure 2c a snapshot of the structure around a cytosine base (residue Cyt8) in which the solvent is illustrated by a surface. As we can see,

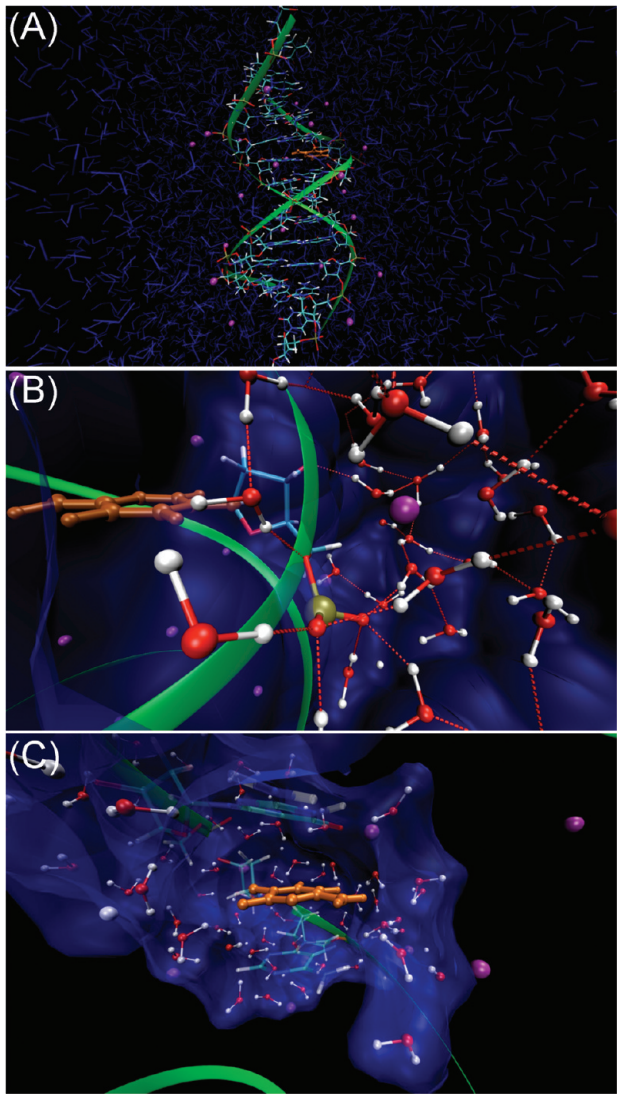

Figure 2. (a) The 12-mer B-DNA fragment plus 22 sodium counterions and 5760 water molecules studied in the QM/MM calculations of this work. (b) Snapshot illustrating the solvation structure around the sodium and phosphate group coordinating a cytosine (residue Cyt8) (c). Snapshot illustrating the hydration environment around a cytosine (residue Cyt8). Atoms O, H, Na, and P are colored in red, white, purple, and tan, respectively.

the DNA fragment that we are interested in is sequestered in the hydrophobic environment of the double helix and is well isolated from the solvent of the MM system, making the contributions from the long-range electrostatic interactions (the first terms in eq 2) between the DNA base (included in the QM region) and MM solvent the largest contribution to the QM/MM interactions. This validates the use of the QM/MM method that provides an accurate account of the effects of the point charges of the MM region.

On the basis of this configuration, optimized geometries of neutral single DNA bases were obtained using a multiregion QM/MM optimization algorithm, which performs a sequence of alternating optimization cycles of the QM and MM regions, as implemented in NWChem.[100] These optimizations were performed, at the B3LYP[101−103] density functional theory (DFT) level of theory and with the aug-cc-pVDZ basis set, using a very limited QM region containing only a single DNA base fragment (Gua9, Ade7, Cyt8, Thy105) for each of the four bases. This choice of the QM region is further discussed in section 3.1. To provide the vertical IP values of the DNA bases, single point QM/MM energy calculations were made with the CCSD(T) theory and the aug-cc-pVDZ basis set. This approach was demonstrated to provide good values of ionization energies for isolated gas-phase nucleic acid bases.[41] The vertical IPs were calculated as the energy difference between the neutral and cation species, both being evaluated at the equilibrium geometry of the neutral state embedded in the equilibrated DNA structure. The energies for the cationic systems were obtained using restricted open-shell wave functions. In order to look at the effects of the DNA solvated environment, gas-phase CCSD(T)/aug-cc-pVDZ IP calculations have also been performed using the neutral DNA base geometries optimized in a vacuum at the DFT B3LYP/aug-cc-pVDZ level of theory.

The QM region, being too restrictive to correctly describe the interactions between DNA bases, has been further enlarged to include clusters of DNA bases of different sizes up to a four-base-pair DNA duplex. In each calculation, the QM region involved the DNA bases with the associated sugar−phosphate groups and sodium ions. The geometries of these clusters have been taken from the MD equilibration procedure with no further optimization. The CCSD(T) method becomes too expensive for the larger π-stacked base and H-bonded base-pair calculations. Therefore, the vertical IPs of these clusters of DNA bases were calculated at the DFT/B3LYP level with the modified 6-31G(d=0.2) basis set. This basis set corresponds to the standard 6-31G basis set augmented by diffuse polarization functions (exponent $\alpha_d = 0.2$) on the heavy atoms: carbon, oxygen, and nitrogen. It has been demonstrated that this basis can be used to predict the H-bond and $\pi-\pi$ energies[104] and to compute the energy differences related to ionization[42] as well as larger polarized and/or augmented basis sets of the literature but at lower computer costs. Finally, further IP calculations have been performed for the four-base-pair duplex: in the gas phase and in interaction with the first hydration shell (48 water molecules). The comparison of the results allowed us to highlight the surprisingly important role played by the DNA environment on ionization energies of bases. Our primary goal in this work was to estimate the influence of long-range solvation interactions on the ionization properties of DNA base clusters rather than provide highly accurate IP evaluations. Thus, for cluster calculations, although there are limitations of the B3LYP exchange correlation functional to describe the dispersion interactions,[105,106] such a method was used as the QM level in these hybrid QM/MM calculations.

3. Results and Discussion

3.1. Single DNA Bases. ***Definition of the QM Region.*** The most difficult problem with the application of a QM/MM method is the definition of the QM and MM regions. If the definition involves the severing of covalent bonds, the development of a reliable QM/MM may become a major problem. In a simple view of the vertical IP calculations, the emitted electron originates from the highest occupied molecular orbital (HOMO). As described above, we chose, in a first step, to use a high-level quantum chemistry method of calculation but restricted the representation of the QM region to the nucleobase only. The accuracy of the QM/MM estimation of the vertical IP is, therefore, related to the localization of the HOMO to the base rather than the sugar moiety or phosphate group. As discussed above in the gas phase, the origin of the lowest vertical IP in the nucleotides remains a somewhat controversial issue. Recently, the vertical IPs of fully solvated pyrimidine nucleosides have been reported by Slavíček et al.[26] These recent direct observations and calculations provide convincing evidence that

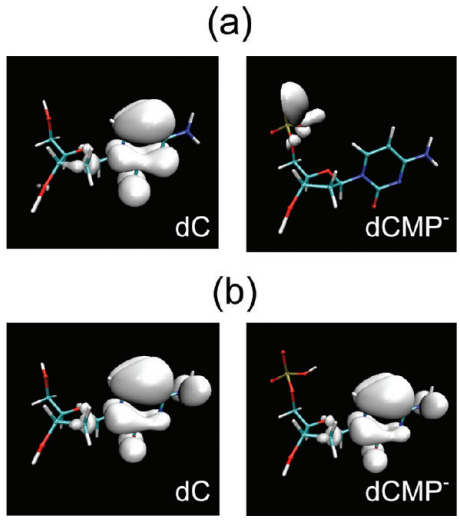

Figure 3. HOMO isosurface obtained at the HF/aug-cc-pVDZ level of theory for cytidine (dC) and 2′-deoxycytidine 5′-monophosphate ($dCMP^-$) (a) in the gas phase and (b) in DNA environment.

TABLE 1: Results of Gas-Phase and QM/MM Calculations of Vertical IPs of DNA Bases (in eV)[a]

	exp. range[b]	CCSD(T)/aug-cc-pVDZ		
DNA base	gas phase	gas phase	QM/MM	Δ
Gua	8.0−8.3	7.93	11.09	3.16
Ade	8.3−8.5	8.23	11.55	3.32
Cyt	8.8−9.0	8.65	11.98	3.33
Thy	9.0−9.2	8.98	12.33	3.35

[a] Energies (Δ) of QM/MM results relative to the calculated gas-phase values are included. Comparison with the gas-phase experimental values. [b] References 4, 6−11, and 13.

hydration of the nucleotides in a homogeneous aqueous environment strongly localizes the excitations in the π structure of the base. However, the solvation structure created by the charged DNA helix and counterions is expected to be different from that of a homogeneous system. To quantify the effect of the DNA environment, we performed calculations in the gas phase and DNA environment on cytidine (dC) and 2′-deoxycytidine 5′-monophosphate ($dCMP^-$). For both, the lowest ionization site has been assigned qualitatively to the HOMO obtained at the HF/aug-cc-pVDZ level of theory. The results of gas-phase and QM/MM calculations are presented in Figure 3a and b, respectively. For dC, the HOMO is on the base both in the gas phase and in the DNA environment. The same result has been obtained for the HOMO of the dC species in water.[26] As suggested in previous work,[71,73] the HOMO of $dCMP^-$ is located, in the gas phase, on the phosphate group. Moving to the solvated DNA environment (Figure 3b), the highest occupied orbital now corresponds to a π-orbital of the cytosine moiety. This effect of the hydrated DNA environment is expected to be similar for all nucleotides, suggesting that the electronic structure changes involved in the lowest energy ionization process of the nucleotides are associated with orbitals strongly localized on the base.

QM/MM Calculations of Ionization Potentials. The vertical IPs of the four individual DNA bases, calculated in the DNA helix structure solvated with 5760 water molecules using the CCSD(T)/MM method with the aug-cc-pVDZ basis set, are collected in Table 1. Results of the gas-phase IP calculations at the same level of theory with geometries optimized in a vacuum are also included in the table where they are compared to the gas-phase experimental values.[4,6−11,13] The gas-phase values are found to be in reasonable agreement (within 0.15 eV) with the corresponding experimental data and are similar (within less than 0.2 eV) to the CCSD(T) results obtained by Roca-Sanjuán et al.[41] The QM/MM vertical IP values calculated for bases in the DNA environment show a large increase of 3.2−3.3 eV compared to the gas phase. Guanine has the lowest IP within the solvated DNA structure, followed by adenine, cytosine, and thymine with IP(Gua) 1.2 eV less than IP(Thy). This result is consistent with previous gas-phase calculations.[41]

TABLE 2: Results of CCSD(T)/aug-cc-pVDZ Calculations of Vertical IPs (in eV) of Cytosine in the Gas Phase (IP_{gas}), in Solution (IP_{aq}), and in the Presence of Unsolvated ($IP_{DNA\text{-}bare}$) and Solvated DNA (IP_{DNA})[a]

cytosine	CCSD(T)	Δ
IP_{gas}	8.55	0.00
IP_{aq}	9.22	0.67
$IP_{DNA\text{-}bare}$	8.32	−0.23
IP_{DNA}	11.98	3.43

[a] Energies (Δ) of QM/MM results relative to the calculated gas-phase value are indicated.

The major effect of the DNA environment on the vertical IPs of DNA bases comes from the electrostatic interactions with the solvating waters in the MM region. To support this conjecture, the vertical IP of cytosine was calculated using reduced regions of the MM space. These results are summarized in Table 2 and include the vertical IP_{gas} calculated for the structure of cytosine optimized in the DNA environment but calculated in the vacuum and the vertical IP values obtained in solution (IP_{aq}) and in the presence of unsolvated ($IP_{DNA\text{-}bare}$) and solvated (IP_{DNA}) DNA. The energies relative to the gas-phase value are also included. Calculation of the vertical IP in the homogeneous liquid shows only a slight increase with IP_{aq} of 9.22 eV which is somewhat larger than the experimental value of 8.3 eV.[26] When computed with the bare DNA helix and counterions, constructed from the optimized solvated DNA complex by removing all of the water molecules, the resulting $IP_{DNA\text{-}bare}$ value of 8.32 eV is similar to the gas-phase IP_{gas} but significantly smaller than the fully hydrated complex, 11.98 eV. The results demonstrate that the significant IP shift compared to the gas-phase value is created by the complex molecular environment of DNA and that the interactions with the solvent structure around the DNA-cation play a key role leading to the high IP values. The IP shift found in this work in the fully solvated DNA environment is significantly larger than the shift reported by Roca-Sanjuán et al. (0.66 eV).[49] A direct comparison is however difficult, since the authors do not give any details about the environment they used, i.e., the size of the solvent box and equilibration. Thus, this difference may be due to a different environment. As has already been demonstrated for the chloride ion and will be shown just below in the case of cytosine, the long-range solvent effects are crucial in determining accurate IP values.

To probe in more detail the influence of the solvation structure on the vertical IPs, we have performed a series of CCSD(T)/MM calculations for the cytosine embedded in the DNA environment with varying solvation controlled by including the water molecules within a distance (d_{solv}) from the DNA helix surface (note that this distance is not the distance from the helix center). The extent of the hydration, colored for each value of d_{solv}, is shown in Figure 4a. The calculated vertical IPs are presented in Figure 4b as a function of the distance d_{solv} ranging from 0 Å (gas phase) to 52 Å (40 000 waters). The number of water molecules implied in each simulation is also plotted. We

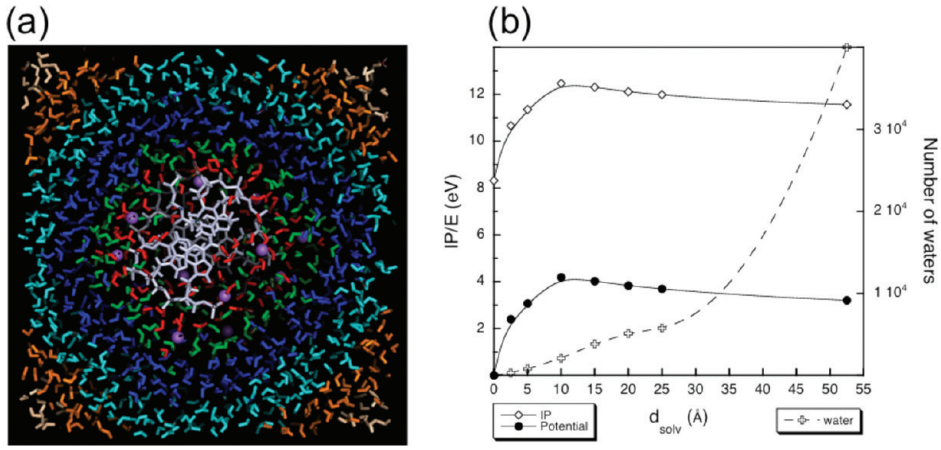

Figure 4. (a) DNA hydrating waters within 2.5, 5, 10, 15, 20, and 25 Å of the DNA helix surface drawn in red, green, dark blue, light blue, orange, and pink, respectively. (b) Vertical IP of cytosine (diamonds) calculated at the CCSD(T)/aug-cc-pVDZ level, electric potential (E) estimated at the center of the DNA base (circles), and number of hydrating waters included in each calculation (crosses) as a function of the distance (d_{solv}) from the DNA surface.

observe a significant change of the IP value between $d_{solv} = 0$ and the maximum value of IP at $d_{solv} = 10$ Å (2100 waters). All of the sodium counterions are found within this radius. Beyond 10 Å, the IP value stabilizes and converges to 11.56 eV for $d_{solv} = 52$ Å (40 000 waters). A similar trend was observed in Figure 1 for the IP of the chloride ion. The electric potential (Coulomb potential) due to the water SPC/E charges in the solvation region calculated at the center of mass of the cytosine base is also provided in Figure 4b as a function of d_{solv}. We observe that the shape of the electric potential curve roughly follows the shape of the IP curve with the maximum at $d_{solv} = 10$ Å. These results are consistent with the notion that the equilibrated DNA helical structure presents an ordered pattern of negative phosphate groups and positive counterions, leading to a long-range structure in the solvent creating an electric potential of considerable magnitude. This potential leads to the elevated vertical IPs reported in Tables 1 and 2.

Since the solvation structure strongly influences the vertical IP of DNA bases, thermal fluctuations in the solvent are expected to broaden the IP spectra. To examine the possible magnitude of this effect, a 100 ps classical MD simulation was performed and the variations in the vertical IP of the cytosine base calculated. For computational efficiency, the IP of the nucleobase was calculated over the classical MD trajectory at 0.5 ps intervals using the QM/MM model at the B3LYP/cc-pVDZ level of theory. At this level of theory, the calculated IP of cytosine in the DNA environment is within 0.3 eV of the corresponding CCSD(T) IP. The distribution of IP is depicted in Figure 5. As expected, the vertical IP of cytosine in the solvated DNA environment is coupled to the thermal fluctuations in the solvent. These fluctuations can result in IP changes of roughly 1 eV on a picosecond time scale. The average IP approaches a value of 11.91 eV.

3.2. Clusters of DNA Bases. In this section, we report the results of the calculations of vertical IPs of DNA base clusters performed in the gas phase and in the DNA environment using the DFT/B3LYP method with the 6-31G(0.2) basis set. For the QM/MM calculations, the QM region was enlarged to accommodate the increased number of π-stacked and H-bonded base pairs. Note that it is difficult to estimate the accuracy of the calculated IP values of DNA base clusters because B3LYP calculations do not take the dispersion attraction into account. Both gas-phase and QM/MM calculations demonstrate however that the base stacking and base pairing interactions lower the

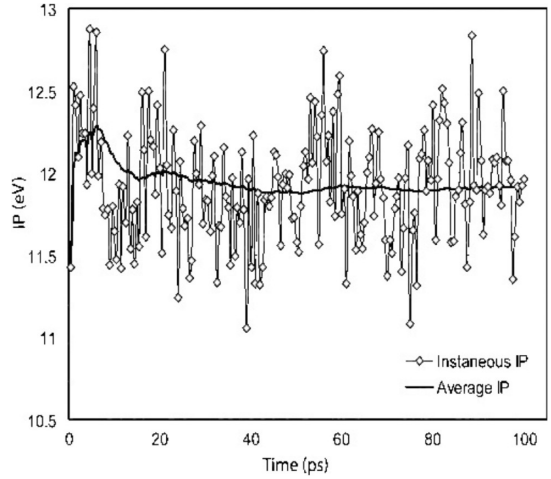

Figure 5. Dynamical evolution of the vertical IP of cytosine in native DNA environment during 100 ps of classical MD simulation resampled with the B3LYP and cc-pVDZ basis set at 0.5 ps intervals. The solid line shows a running average.

IPs, as has been predicted by previous quantum chemistry calculations performed at a higher level of theory.[42,43,47] As demonstrated above for the four isolated DNA bases, our results on the clusters of DNA bases support the fact that, when passing from the gas phase to the DNA environment, the IP of the system changes significantly, up to 4 eV. We will show below that this influence of solvation is found to be not a short- but a long-range effect. We present in Figure 6 the vertical IPs of six DNA base complexes calculated in the solvated DNA environment. The B3LYP/6-31G(0.2) results for the single-stranded oligonucleotides d(5′-C_8G_9-3′), d(5′-$C_8G_9C_{10}$-3′), and d(5′-$A_7C_8G_9C_{10}$-3′) are presented by solid lines in columns a, b, and c, respectively. For reference, the vertical IP of the single guanine base G_9 calculated at the same level of theory is also given. Dotted lines represent the results of QM/MM IP calculations in which the opposite strands of the DNA duplex are included in the QM region. In each cluster calculation, the QM region, shown in Figure 6, involves the DNA bases, the sugar−phosphate groups with the associated sodium ions, and hydrogen link atoms (two per strand). The MM region contains the rest of the DNA 12-mer fragment, the counterions, and the solvent molecules (5760 water molecules). The results obtained in the DNA environment show that the IP value for the oligonucleotide d(5′-C_8G_9-3′) is 0.95 eV smaller than that for

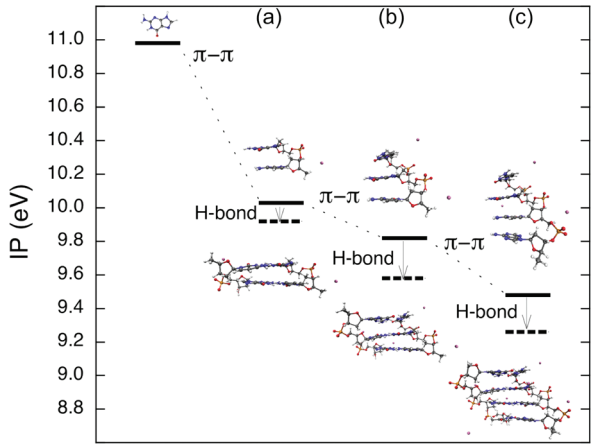

Figure 6. Vertical IPs of six DNA base complexes calculated in the solvated DNA environment, using the B3LYP method with the 6-31G(0.2) basis set. The solid lines in columns a, b, and c provide the results of the calculations where the QM region consisted of single-stranded oligonucleotides d(5′-C_8G_9-3′), d(5′-$C_8G_9C_{10}$-3′), and d(5′-$A_7C_8G_9C_{10}$-3′), respectively (see inset). Dotted lines present the results where the opposite stands of the DNA duplex are included in the QM region. For reference, the vertical IP of the single guanine base G_9 calculated at the same level of theory is also given.

TABLE 3: Results of B3LYP/6-31G(0.2) Calculations of Vertical IPs (in eV) of the Configuration of the Isolated Four-Base-Pair B-DNA Duplex d(5′-$A_7C_8G_9C_{10}$-3′) in the Gas Phase (IP_{gas}) and in the Presence of the First Hydration Shell Treated at the MM ($IP_{1st\ shell\text{-}MM}$) or QM ($IP_{1st\ shell\text{-}QM}$) Level[a]

4-bp duplex	B3LYP	Δ
IP_{gas}	5.24	0.00
$IP_{first\ shell\text{-}MM}$	5.27	0.07
$IP_{first\ shell\text{-}QM}$	5.31	0.03
IP_{DNA}	9.26	4.02

[a] The value calculated in the solvated DNA environment is also provided (IP_{DNA}). Energies (Δ) relative to the gas-phase IP are included.

the isolated guanine. DNA base stacking along a single strand lowers clusters' vertical IP further by 0.2−0.3 eV, while the formation of H-bonded base pairs affects the ionization energies by 0.1−0.2 eV. These values are consistent with the recent high-level EOM-CCSD calculations reported by Golubeva et al.[47] The minimum IP is obtained for the four-base-pair duplex. For this system, the vertical IP in the DNA environment (IP_{DNA}) is found to be 9.26 eV. The gas-phase vertical IP_{gas} value of the same structure is 5.24 eV, resulting in a shift of 4.02 eV compared to the solvated DNA environment, qualitatively similar to the shifts reported for single bases in Table 1.

While there are no measurements of the IP of DNA oligomers in the solution phase, we performed full QM calculations on the four-base-pair duplex, d(5′-$A_7C_8G_9C_{10}$-3′), configuration using the B3LYP level of approximation to provide a test of the accuracy of the QM/MM separation of the system into QM and MM parts. With this objective, we investigated the ionization energy of the B-DNA duplex interacting with the first solvation shell (48 waters). The results are presented in Table 3 in which the IPs calculated in the gas phase and the DNA environment are also provided. Adding the first 48 waters of hydration and treating all of the atoms at the B3LYP level changes the vertical IP only slightly compared to the gas phase, $IP_{first\ shell\text{-}QM} = 5.31$ eV. If the hydrating waters are treated at the MM level, the IP of the hydrated configuration ($IP_{first\ shell\text{-}MM}$) is found to produce a very similar value of 5.27 eV, supporting the accuracy of the QM/MM method for this calculation. The very small IP shift of the microsolvated system (48 waters) relative to the gas phase found in this work differs from the DFT/BLYP results reported by Barnett et al.[65] for the four-base-pair B-DNA duplex d(5′-GAGG-3′) plus 48 hydrating waters and sodium counterions who predict an increase in the vertical IP of 1.3 eV on the inclusion of the first hydration shell. After having performed test calculations, we saw that this difference is not due to the different levels of approximation used. However, this difference may be caused by differences in the structure (e.g., the DNA sequence and the position of the sodium counterions). Moreover, we saw that the thermal fluctuations in the solvent can result in changes in the IP of DNA bases of roughly 1 eV. Given this, our result appears to be consistent with the value obtained by these authors.

4. Conclusions

The vertical ionization potentials (IPs) of nucleobases in the DNA environment have been studied by means of QM/MM calculations. The accuracy of the QM/MM method for vertical IP calculations was tested for the Cl^- ion in the gas phase and the aqueous phase. The QM/MM model used in this work is justified by a clear separation of the solvent charges of the MM region from the bases situated inside the DNA helix structure. As expected from previous investigations,[78−80] we demonstrate that, unlike in the gas phase, the DNA polar surroundings favor the charge localization on the base rather than the sugar moiety or phosphate group. Therefore, in a first step, each of the four single bases were individually chosen to be included in the QM region and calculated at a high level of theory, CCSD(T)/aug-cc-pVDZ. The remaining 12-mer B-DNA fragment, counterions, and water solvent molecules (5760 SPC/E waters) were defined as the MM region. The entire system was equilibrated to 298.15 K. The calculated vertical IPs of the DNA bases show an unexpectedly large positive shift of roughly 3.2−3.3 eV from the corresponding gas-phase values. The shift is found to be nearly the same for all four DNA bases. The IP variation of the cytosine base with thermal fluctuations in the solvent has been examined. Changes in IP of roughly 1 eV on a picosecond time scale have been obtained. IPs of π-stacked and H-bonded clusters of DNA bases were, in a second step, also calculated using the same QM/MM model but with a lower level of theory, B3LYP/6-31G(d=0.2). An IP shift of 4.02 eV relative to the gas phase is found for a four-base-pair B-DNA duplex configuration. Our calculations demonstrate that increased vertical IP values of DNA bases and clusters of DNA bases are due to the presence of an electric potential created by the structure of the MM solvent. The ordered pattern of negative phosphate groups and positive counterions in the DNA helix induces long-range structure in the solvent which in turn creates a significant electric potential at the site of the base fragment.

The present findings point to an interesting phenomenon where long-range modulation of the solvent structure strongly affects the ionization properties of DNA bases. Therefore, we highlight the importance of an explicit molecular description of the solvation region in the QM/MM approach, which is a very significant advantage over the continuum models, to provide a predictive capability for ionization of DNA components showing that the charged nature of the double helix is crucial in producing an accurate model of the hydrated DNA environment. The IP shifts that we calculated here must be considered in the extrapolation of experimental observations

from the gas or homogeneous phase. This result is of extreme relevance to understanding the role that the DNA environment plays in ionization.

Acknowledgment. E.C. thanks the Belgian American Educational Foundation (B.A.E.F.) for a postdoc fellowship and the F.R.S.-FNRS (Fonds National de la Recherche Scientifique de Belgique). A portion of this work was supported by DOE BES grant #DE-FG02-06ER15767 and NSF grant #EAR0545811. Support to M.V. from DOE ASCR Multiscale Mathematics program and Office of Naval Research is gratefully acknowledged. The work at Pacific Northwest National Laboratory (PNNL) was supported by the U.S. Department of Energy (DOE), Office of Basic Energy Sciences, Chemical Sciences, Geosciences, and Biosciences Division. Computational resources were provided by the Molecular Science Computing Facility (MSCF) in the William R. Wiley Environmental Molecular Sciences Laboratory (EMSL) funded by DOE's Office of Biological and Environmental Research. Battelle operates PNNL for DOE under contract DE-AC06-76RLO-1830. Discussions with Karol Kowalski are much appreciated. Stephen E. Bradforth is acknowledged for helpful discussions.

References and Notes

(1) Cadet, J.; et. al. *Redox Genome Interactions in Health and Disease*; Marcel Dekker: New York, 2003; Chapter 8.

(2) *Theory of the interaction of radiation with biomolecules*; Sabin, J. R., Ed.; Advances in Quantum Chemistry, Vol. 52; Elsevier/Academic Press: Amsterdam, The Netherlands, 2007.

(3) Shikazono, N.; Noguchi, M.; Fujii, K.; Urushibara, A.; Yokoya, A. *J. Radiat. Res.* **2009**, *50*, 27.

(4) Hush, N. S.; Cheung, A. S. *Chem. Phys. Lett.* **1975**, *34*, 11.

(5) Orlov, V. M.; Smirnov, A. N.; Varshavsky, Y. M. *Tetrahedron Lett.* **1976**, *48*, 4377.

(6) Padva, A.; O'Donnell, T. J.; LeBreton, P. R. *Chem. Phys. Lett.* **1976**, *41*, 278.

(7) Dougherty, D. A.; McGlynn, S. P. *J. Chem. Phys.* **1977**, *67*, 1289.

(8) Dougherty, D. A.; Younathan, E. S.; Voll, R.; Abdulnur, S.; McGlynn, S. P. *J. Electron Spectrosc. Relat. Phenom.* **1978**, *13*, 379.

(9) Yu, C.; Peng, S.; Akiyama, I.; Lin, J.; LeBreton, P. R. *J. Am. Chem. Soc.* **1978**, *100*, 2303.

(10) Lin, J.; Yu, C.; Peng, S.; Akiyama, I.; Li, K.; Lee, L. K.; LeBreton, P. R. *J. Phys. Chem.* **1980**, *84*, 1006.

(11) Lin, J.; Yu, C.; Peng, S.; Akiyama, I.; Li, K.; Lee, L. K.; LeBreton, P. R. *J. Am. Chem. Soc.* **1980**, *102*, 4627.

(12) Lias, S. G.; Bartmess, J. E.; Liebman, J. F.; Holmes, J. L.; Levin, R. D.; Mallard, W. G. *J. Phys. Chem. Ref. Data* **1988**, *17*, 1.

(13) Urano, S.; Yang, X.; LeBreton, P. R. *J. Mol. Struct.* **1989**, *214*, 315.

(14) Kim, S. K.; Lee, W.; Herschbach, D. R. *J. Phys. Chem.* **1996**, *100*, 7933.

(15) Schiedt, J.; Weinkauf, R.; Neumark, D. M.; Schlag, E. W. *Chem. Phys.* **1998**, *239*, 511.

(16) Kim, N. J.; Kang, H.; Jeong, G.; Kim, Y. S.; Lee, K. T.; Kim, S. K. *J. Phys. Chem. A* **2000**, *104*, 6552.

(17) Piuzzi, F.; Mons, M.; Dimicoli, I.; Tardivel, B.; Zhao, Q. *Chem. Phys.* **2001**, *270*, 205.

(18) Papadantonakis, G. A.; Tranter, R.; Brezinsky, K.; Yang, Y.; van Breemen, R. B.; LeBreton, P. R. *J. Phys. Chem. B* **2002**, *106*, 7704.

(19) Kim, N. J.; Kim, Y. S.; Jeong, G.; K., A. T.; Kim, S. K. *Int. J. Mass Spectrom.* **2002**, *219*, 11.

(20) Kang, H.; Lee, K. T.; Kim, S. K. *Chem. Phys. Lett.* **2002**, *359*, 213.

(21) Crews, B.; Abo-Riziq, A.; Grace, L.; Callahan, M.; Kabelac, M.; Hobza, P.; de Vries, M. S. *Phys. Chem. Chem. Phys.* **2005**, *7*, 3015.

(22) Choi, K.-W.; Lee, J.-H.; Kim, S. K. *J. Am. Chem. Soc.* **2005**, *127*, 15674.

(23) Jochims, H.-W.; Schwell, M.; Baumgärtel, H.; Leach, S. *Chem. Phys.* **2005**, *314*, 263.

(24) Belau, L.; Wilson, K. R.; Leone, S. R.; Ahmed, M. *J. Phys. Chem. A* **2007**, *111*, 7562.

(25) Zavilopulo, A. N.; Shpenik, O. B.; Agafonova, A. S. *J. Phys. B: At. Mol. Opt. Phys.* **2009**, *42*, 025101.

(26) Slavíček, P.; Winter, B.; Faubel, M.; Bradforth, S. E.; Jungwirth, P. *J. Am. Chem. Soc.* **2009**, *131*, 6460.

(27) Sevilla, M. D.; Besler, B.; Colson, A. O. *J. Phys. Chem.* **1995**, *99*, 1060.

(28) Improta, R.; Scalmani, G.; Barone, V. *Int. J. Mass Spectrom.* **2000**, *201*, 321.

(29) Wetmore, S. D.; Boyd, R. J.; Eriksson, L. A. *Chem. Phys. Lett.* **2000**, *322*, 129.

(30) Dolgounitcheva, O.; Zakrzewski, V. G.; Ortiz, J. V. *Int. J. Quantum Chem.* **2000**, *80*, 831.

(31) Dolgounitcheva, O.; Zakrzewski, V. G.; Ortiz, J. V. *J. Am. Chem. Soc.* **2000**, *122*, 12304.

(32) Dolgounitcheva, O.; Zakrzewski, V. G.; Ortiz, J. V. *J. Phys. Chem. A* **2002**, *106*, 8411.

(33) Dolgounitcheva, O.; Zakrzewski, V. G.; Ortiz, J. V. *J. Phys. Chem. A* **2003**, *107*, 822.

(34) Hanus, M.; Ryjacek, F.; Kabelac, M.; Kubar, T.; Bogdan, T. V.; Trygubenko, S. A.; Hobza, P. *J. Am. Chem. Soc.* **2003**, *125*, 7678.

(35) Close, D. M. *J. Phys. Chem. B* **2003**, *107*, 864.

(36) Close, D. M. *J. Phys. Chem. A* **2004**, *108*, 10376.

(37) Crespo-Hernàndez, C. E.; Arce, R.; Ishikawa, Y.; Gorb, L.; Leszczynski, J.; Close, D. M. *J. Phys. Chem. A* **2004**, *108*, 6373.

(38) Gomzi, V.; Herak, J. N. *THEOCHEM* **2004**, *683*, 155.

(39) Close, D. M.; Crespo-Hernàndez, C. E.; Gorb, L.; Leszczynski, J. *J. Phys. Chem. A* **2005**, *109*, 9279.

(40) Close, D. M.; Crespo-Hernàndez, C. E.; Gorb, L.; Leszczynski, J. *J. Phys. Chem. A* **2006**, *110*, 7485.

(41) Roca-Sanjuán, D.; Rubio, M.; Merchán, M.; Serrano-Andrés, L. *J. Chem. Phys.* **2006**, *125*, 084302.

(42) Cauët, E.; Dehareng, D.; Liévin, J. *J. Phys. Chem. A* **2006**, *110*, 9200.

(43) Cauët, E.; Liévin, J. *Adv. Quantum Chem.* **2007**, *52*, 121.

(44) Close, D. M.; Crespo-Hernàndez, C. E.; Gorb, L.; Leszczynski, J. *J. Phys. Chem. A* **2008**, *112*, 4405.

(45) Close, D. M.; Crespo-Hernàndez, C. E.; Gorb, L.; Leszczynski, J. *J. Phys. Chem. A* **2008**, *112*, 12702.

(46) Close, D. M.; Øhman, K. T. *J. Phys. Chem. A* **2008**, *112*, 11207.

(47) Golubeva, A. A.; Krylov, A. I. *Phys. Chem. Chem. Phys.* **2009**, *11*, 1303.

(48) Sun, L. X.; Bu, Y. X. *THEOCHEM* **2009**, *909*, 25.

(49) Roca-Sanjuán, D.; Olaso-González, G.; Rubio, M.; Coto, P. B.; Merchán, M.; Ferré, N.; Ludwig, V.; Serrano-Andrés, L. *Pure Appl. Chem.* **2009**, *81*, 743.

(50) Colson, A. O.; Besler, B.; Close, D. M.; Sevilla, M. D. *J. Phys. Chem.* **1992**, *96*, 661.

(51) Colson, A. O.; Besler, B.; Sevilla, M. D. *J. Phys. Chem.* **1993**, *97*, 13852.

(52) Hutter, M.; Clark, T. *J. Am. Chem. Soc.* **1996**, *118*, 7574.

(53) Bertran, J.; Oliva, A.; Rodriguez-Santiago, L.; Sodupe, M. *J. Am. Chem. Soc.* **1998**, *120*, 8159.

(54) Li, X.; Cai, Z.; Sevilla, M. D. *J. Phys. Chem. B* **2001**, *105*, 10115.

(55) Li, X.; Cai, Z.; Sevilla, M. D. *J. Phys. Chem. A* **2002**, *106*, 9345.

(56) Sugiyama, H.; Saito, I. *J. Am. Chem. Soc.* **1996**, *118*, 7063.

(57) Prat, F.; Houk, K. N.; Foote, C. S. *J. Am. Chem. Soc.* **1998**, *120*, 845.

(58) Saito, I.; Nakamura, T.; Nakatani, K.; Yoshioka, Y.; Yamaguchi, K.; Sugiyama, H. *J. Am. Chem. Soc.* **1998**, *120*, 12686.

(59) Yoshioka, Y.; Kitagawa, Y.; Takano, Y.; Yamaguchi, K.; Nakamura, T.; Saito, I. *J. Am. Chem. Soc.* **1999**, *121*, 8712.

(60) Voityuk, A. A.; Jortner, J.; Bixon, M.; Rösch, N. *Chem. Phys. Lett.* **2000**, *324*, 430.

(61) Schumm, S.; Prévost, M.; Garcia-Fresnadillo, D.; Lentzen, O.; Moucheron, C.; Kirsch-De Mesmaeker, A. *J. Phys. Chem. B* **2002**, *106*, 2763.

(62) Kim, H. S.; LeBreton, P. R. *Proc. Natl. Acad. Sci. U.S.A.* **1994**, *91*, 3725.

(63) Kim, N. S.; Zhu, Q.; LeBreton, P. R. *J. Am. Chem. Soc.* **1999**, *121*, 11516.

(64) Zhu, Q.; LeBreton, P. R. *J. Am. Chem. Soc.* **2000**, *122*, 12824.

(65) Barnett, R. N.; Cleveland, C. L.; Joy, A.; Landman, U.; Schuster, G. B. *Science* **2001**, *294*, 567.

(66) Barnett, R. N.; Cleveland, C. L.; Landman, U.; Boone, E.; Kanvah, S.; Schuster, G. B. *J. Phys. Chem. A* **2003**, *107*, 3525.

(67) Kim, S.; Schaefer, H. F. *J. Phys. Chem. A* **2007**, *111*, 10381.

(68) Tomasi, J.; Mennucci, B.; Cancès, E. *THEOCHEM* **1999**, *464*, 211.

(69) Cossi, M.; Barone, V. *J. Phys. Chem. A* **2000**, *104*, 10614.

(70) Cossi, M.; Barone, V. *J. Chem. Phys.* **2000**, *112*, 2427.

(71) Yang, X.; Wang, X. B.; Vorpagel, E. R.; Wang, L. S. *Proc. Natl. Acad. Sci. U.S.A.* **2004**, *101*, 17588.

(72) Hou, R.; Gu, J.; Xie, Y.; Yi, X.; Schaefer, H. F., III. *J. Phys. Chem. B* **2005**, *109*, 22053.

(73) Zakjevskii, V. V.; King, S. J.; Dolgounitcheva, O.; Zakrzewski, V. G.; Ortiz, J. V. *J. Am. Chem. Soc.* **2006**, *128*, 13350.

(74) Rubio, M.; Roca-Sanjuán, D.; Merchán, M.; Serrano-Andrés, L. *J. Phys. Chem. B* **2006**, *110*, 10234.
(75) Close, D. M. *J. Phys. Chem. A* **2008**, *112*, 8411.
(76) Rubio, M.; Roca-Sanjuán, D.; Serrano-Andrés, L.; Merchán, M. *J. Phys. Chem. B* **2009**, *113*, 2451.
(77) Magulick, J.; Beerbom, M. M.; Schlaf, R. *Thin Solid Films* **2008**, *516*, 2396.
(78) Kim, H. S.; LeBreton, P. R. *J. Am. Chem. Soc.* **1996**, *118*, 3694.
(79) Kim, N. S.; LeBreton, P. R. *Biospectroscopy* **1997**, *3*, 1.
(80) Fernando, H.; Papadantonakis, G. A.; Kim, N. S.; LeBreton, P. R. *Proc. Natl. Acad. Sci. U.S.A.* **1998**, *95*, 5550.
(81) Valiev, M.; Kowalski, K. *J. Chem. Phys.* **2006**, *125*, 211101.
(82) Epifanovsky, E.; Kowalski, K.; Fan, P. D.; Valiev, M.; Matsika, S.; Krylov, A. I. *J. Phys. Chem. A* **2008**, *112*, 9983.
(83) Kowalski, K.; Valiev, M. *J. Phys. Chem. A* **2008**, *112*, 5538.
(84) Grossfield, A.; Ren, P.; Ponder, J. W. *J. Am. Chem. Soc.* **2003**, *125*, 15671.
(85) Jorgensen, W. L. *J. Chem. Theory Comput.* **2007**, *3*, 1877.
(86) Fanourgakis, G. S.; Xantheas, S. S. *J. Chem. Phys.* **2008**, *128*, 074506.
(87) Lin, H.; Truhlar, D. G. *Theor. Chem. Acc.* **2007**, *117*, 185.
(88) Markovich, G.; Pollack, S.; Giniger, R.; Cheshnovsky, O. *J. Chem. Phys.* **1994**, *101*, 9344.
(89) Winter, B.; Weber, R.; Hertel, I. V.; Faubel, M.; Jungwirth, P.; Brown, E. C.; Bradforth, S. E. *J. Am. Chem. Soc.* **2005**, *127*, 7203.
(90) Berendsen, H. J. C.; Grigera, J. R.; Straatsma, T. P. *J. Phys. Chem.* **1987**, *91*, 6269.
(91) Cornell, W. D.; Cieplak, P.; Bayly, C. I.; Gould, I. R.; Merz, K. M.; Ferguson, D. M.; Spellmeyer, D. C.; Fox, T.; Caldwell, J. W.; Kollman, P. A. *J. Am. Chem. Soc.* **1995**, *117*, 5179.
(92) Watts, J. P.; Gauss, J.; Bartlett, R. J. *J. Chem. Phys.* **1993**, *98*, 8718.
(93) Kendall, R. A.; Dunning, T. H. J.; Harrison, R. J. *J. Chem. Phys.* **1992**, *96*, 6796.
(94) Jagoda-Cwiklik, B.; Slavíček, P.; Cwiklik, L.; Nolting, D.; Winter, B.; Jungwirth, P. *J. Phys. Chem. A* **2008**, *112*, 3499.
(95) Krekeler, C.; Hess, B.; Delle Site, L. *J. Chem. Phys.* **2006**, *125*, 054305.
(96) Krekeler, C.; Delle Site, L. *J. Phys.: Condens. Matter* **2007**, *19*, 192101.
(97) Guàrdia, E.; Skarmoutsos, *J. Chem. Theory Comput.* **2009**, *5*, 1449.
(98) Zhao, Z.; Rogers, D. M.; Beck, T. L. *J. Chem. Phys.* **2010**, *132*, 014502.
(99) Wasserman, E.; Wood, B.; Brodhol, J. *Geochim. Cosmochim. Acta* **1995**, *59*, 1.
(100) Valiev, M.; Garrett, B. C.; Tsai, M. K.; Kowalski, K.; Kathmann, S. M.; Schenter, G. K.; Dupuis, M. *J. Chem. Phys.* **2007**, 127.
(101) Becke, A. D. *Phys. Rev. A* **1988**, *38*, 3098.
(102) Lee, C.; Yang, W.; Parr, R. G. *Phys. Rev. B* **1988**, *37*, 785.
(103) Becke, A. D. *J. Chem. Phys.* **1993**, *98*, 5648.
(104) Wintjens, R.; Biot, C.; Rooman, M.; Liévin, J. *J. Phys. Chem. A* **2003**, *107*, 6249.
(105) Tsuzuki, S.; Lüthi, H. P. *J. Chem. Phys.* **2001**, *114*, 3949.
(106) Zhao, Y.; Truhlar, D. G. *Phys. Chem. Chem. Phys.* **2005**, *7*, 2701.

JP9120723